NIST-GCR-96-704

FLAME BASE STRUCTURE OF SMALL-SCALE POOL FIRES

S. Venkatesh, A. Ito, K. Saito

Department of Mechanical Engineering
University of Kentucky
Lexington, KY 40506-0108

and

I.S. Wichman

Department of Mechnaical Engineering
Michigan State University
East Lansing, MI 48824-1226

December 1996

U.S. Department of Commerce
Michael Kantor, *Secretary*
Technology Administration
Mary L. Good, *Under Secretary for Technology*
National Institute of Standards and Technology
Arati Prabhakar, *Director*

The Measurement of Transient 2–D Profiles of Velocity and Fuel–Concentration over Liquids

A. Ito*, A. Narumi, T. Konishi*,**
G. Tashtoush, K. Saito and C.J. Cremers

Dept. of Mechanical Engineering
University of Kentucky
Lexington, KY 40506–0108

ABSTRACT

We recently developed two different optical techniques in order to simultaneously measure transient 2–D profiles of velocity, temperature and fuel concentration which were generated by a spreading flame over liquids. The first technique, PTLS, employs a particle–track system combined with a laser–sheet system and a high speed camera, while the second technique employs a dual wavelength holographic interferometer (DWHI). The PTLS system revealed transient 2 D profiles of flame induced flow, while DWHI revealed 2 D profiles of fuel concentration over liquids. In this paper we present a series of velocity profiles for a pulsating flame spread over propanol and concentration profiles for gaseous propanol determined with PTLS and DWHI respectively. Other researchers have predicted the formation of small twin circulations, one a gas–phase circulation just ahead of the flame's leading edge, and the other a small liquid circulation just underneath the gas–phase circulation. Our PTLS results confirmed these predictions, i.e., the formation of a millimeter–diameter circulation in the gas phase and an accompanying liquid flow. Based on these data, we offer a phenomenological explanation of the mechanism of pulsating flame spread. In addition, we show that DWHI is a very promising technique for measuring transient fuel–concentration profiles over liquids.

Present Addresses:

A. Ito and T. Konishi, Dept. of Production Systems Engineering, Oita University, Oita 870–11, Japan, and

A. Narumi, Dept. of Mechanical Engineering, Kanagawa Inst. of Tech., Atsugi, Japan.

INTRODUCTION

Historical Background

The phenomenon of flame spread over liquids is of current interest because of its importance to fire safety. Our objective is different. We wish to learn more about the fundamental mechanism of the flame spread. An excellent review of the literature on this problem was published by Ross [1] and Hirano and Suzuki [2] and the theoretical background of the problem was provided by Williams [3]. They addressed many of the problems that needed to be investigated.

The present paper is a continuation of our previous studies on flame spread over liquids [4–6]. In these studies we applied holographic interferometry (HI) to obtain a detailed and instantaneous temperature distribution in the liquid phase near the fuel surface. In each of methanol, ethanol and propanol we found subsurface–liquid convection in both the uniform spread, and pulsating spread regions. To understand the mechanisms of flame spread in both regions, researchers tried to identify the major heat–transfer process between the flame's leading edge and the liquid, whether it occurs through the gas phase, liquid phase or both. When the liquid convection is produced and it travels ahead of the flame's leading edge, the flame spread is likely to be controlled by it because the convection carries the high temperature liquid ahead of the flame's leading edge. This enhances evaporation of liquid vapor resulting in the formation of a flammable mixture of fuel and air through which the flame can spread. If there is no liquid convection ahead of the flame's leading edge, the major heat transfer can occur between the flame's leading edge and the liquid by conduction and radiation in the gas phase, because conduction through the liquid is negligible [7].

Liquid convection is unique to flame spread over liquids and it complicates the spreading process in comparison to flame spread over solids, which have no condensed phase convection. Thus, it is important to measure temperature and velocity profiles in the liquid phase. Akita [8] was the first researcher to apply a shadowgraph technique to visualize the liquid convection. He reported the formation of liquid convection in the pulsating region, but no liquid convection in the uniform spread region. Based on Akita's data, Glassman and Dryer [7] proposed that the uniform spread is controlled by heat conduction through the gas phase, while in the pulsating region the liquid convection plays an important role. However, the proposed mechanism for the uniform spread is questionable, because the gas–phase conduction may not transfer sufficient heat for the flame to spread at a rate of nearly 10 cm/s.

To solve this problem, we developed an HI system and performed the transient measurement of liquid temperature [4]. The response time of our HI system is less than 1 microsecond. We estimate the uncertainty of the spatial resolution to be $\pm$ 0.1 mm, and the temperature resolution to be $\pm$ 0.1 ^{O}C [4]. Using the HI system, we observed a large liquid convection both in the uniform and pulsating spread regions. The liquid convection in the uniform spread region was a surprise, because the head of the liquid convection preceded the flame's leading edge by approximately 1 cm [4], which is entirely different from Akita's result [8]. To make sure of the accuracy of the data, we repeated the experiments several times and found the reproducibility to be within $\pm$90 %. Thus, we proposed a new mechanism: the flame spread in the uniform spread region is governed by the liquid convection [4]. However, at that time we did not really understand why Akita's shadowgraph results were so different from our HI results.

Later, Howard Ross's group at NASA Lewis Research Center applied rainbow schlieren deflectometry (RSD) to measure liquid convection generated by the spreading flame [9]. They found little liquid convection ahead of the flame's leading edge in the uniform spread region. Their RSD data were similar to Akita's shadowgraphs and disagreed with our HI results. Over the past three years, both NASA and our group have tried to understand the reasons for the disagreement, but failed to do so until a series of parametric experiments was completed. In those experiments, the effects of six different parameters were investigated: sensitivity of both RSD and HI systems, impurity of propanol (if any), the relative humidity of the air, the ambient air temperature, several different types of ignition method, and finally different tray widths. We found that the first five parameters had little influence on the disagreement. However, when we checked the effect of tray width (0.5, 1, and 2 cm) on the liquid convection, the least suspected parameter, a surprising result emerged: the 0.5 cm wide tray had a large liquid convection in the uniform spread region, while the trays that were 1 cm and 2 cm wide had a thin layer of liquid convection. It was so thin and small that only a very sensitive measurement technique could detect it. The result for the 2–cm tray was very similar to the NASA's result for the 2–cm tray. A closer look at their RSD result also revealed a small and thin layer of liquid convection that was always ahead of the flame's leading edge. Comparison of these findings led us to the agreement that in the uniform spread region there is always a small liquid convection indicating that the major heat transfer is by that mode. It also became clear that the shadowgraph [8] did not detect the liquid convection because the size of the liquid convection was too small and beyond the limitation of the spatial resolution of the shadowgraph. Later we applied the shadowgraph technique and proved this explanation.

The validity of this new mechanism has already been proven for the tray that is 0.5 cm wide [4] and extended to one that is 4 cm wide. Beyond that width there are no experimental data, but we speculate that the mechanism will be sustained up to a certain tray width; a hypothesis that will be investigated in the future by both NASA and our group. In the end, both NASA and our group shared Neils Bohr's message "We will never understand anything until we have some contradictions."

Howard Ross's group is now conducting a series of experiments on flame spread using 2 and 4 cm wide trays under the microgravity condition. They have already obtained interesting results which are yet ready to be interpreted [10]. Our group is also conducting a series of flame–spread experiments using 0.5, 1, 2, 4, and 10 cm wide trays under normal gravity.

The Current Problem

NASA's microgravity test results showed that pulsating spread did not occur in either shallow or deep pool experiments [1]; instead the flame was extinguished, indicating the importance of the buoyancy effect in the gas phase on the mechanism of pulsation. Schiller and Sirignano, using numerical calculations [11], predicted the existence of a very small circulation in the gas phase ahead of the flame's leading edge. They suggested that the gas–phase circulation, which is unique in the pulsating spread and appears with the liquid–phase circulation, may play an important role in flame pulsation [11,12]. There are LDV flow measurement data obtained with Laser–Doppler Velocimetry (LDV) by Santoro et al. [13] showing a gas–phase circulation of approximately 1–cm diameter in the pulsating spread region. However, their LDV result is rather a qualitative indication of the formation of circulation.

To confirm the prediction [11,12] and understand the role of the small gas–phase circulation in the flame pulsation, transient velocity profiles in the gas phase just above the liquid surface and just ahead of the flame's leading edge must be measured. These measurements are not easy, because the rate of flame spread varies from a few centimeters to a few tens of centimeters per second and the target region, where detailed velocity profiles are needed, is at most a few millimeters in diameter.

Previously we learned that LDV was not sufficiently accurate for our measurements [14]. Instead we used PTLS to measure flow profiles in 2D with a spatial resolution on the order of a millimeter in the primary anchoring region of a small pool fire [14]. Based on that experience, we applied the same technique to measure a time series of detailed velocity profiles in the pulsating spread region. As a result, we confirmed the formation of a small circulation approximately in the same location as predicted by the UCI numerical model [11]. We also confirmed, in agreement with the model prediction, that the formation of a small circulation appeared only in the pulsating spread region.

To further advance our understanding of the flame spread over liquids, the direct measurement of propanol concentration over the liquid just ahead of the flame's leading edge was conducted using DWHI. Our DWHI data are accurate when the flow of the gas phase flow has a 2–D profile. When the flow profile shifts from the 2D to 3D, our current

DWHI system will lose its accuracy. To overcome this limitation, we are working on the development of an advanced 3–D–DWHI system.

EXPERIMENTAL METHODS

Test Apparatus for Flame Spread

The flame–spread apparatus (Fig. 1) used for this study is essentially the same as that used in a previous flame–spread study [4–6]. A Pyrex tray with variable width (0.5, 1, 2, and 4 cm) x 2 cm deep x 30 cm long was used. The two long sides of the fuel tray were made of Pyrex of 0.2–cm thickness. The entire liquid tray was enclosed in an open top Pyrex test cell 14 cm high x 15 cm wide x 35 cm long in order to minimize laboratory draft and provide a repeatable flame–spread condition.

Propanol was used as fuel, since it provides a common database for us to use for comparison of our data with NASA's microgravity data [1,9] and our previous experiments [4–6]. The fuel was uniformly ignited at one end by a small pilot flame. To measure the velocity of the liquid convection, we sprinkled aluminum particles of 5–μm–diameter onto the liquid surface. That the aluminum particles float on the liquid surface and follow closely the direction of the liquid–flow convection was confirmed by comparing a time series of simultaneous interferograms for both gas and liquid phases with the video taped behavior of the aluminum particles [5]. A chromel–alumel thermocouple with a 50–μm diameter was used to measure the initial liquid temperature. High pressure nitrogen was supplied from a nitrogen cylinder to extinguish the flame. The talc–particle feeding system is the same as the one used in the previous study [14].

Velocity Measurement with a Particle Track and Laser Sheet System (PTLS)

From our previous studies [14,15], we learned that a PTLS technique with a high speed video camera having a speed of 5,000 frames/s and a view angle of 25 degrees can best serve our measurements. The PTLS can measure profiles of both stream lines and 2–D velocity profiles with significantly fewer particles and nearly instantaneously. Using a

6–W Ar–ion laser–beam and a cylindrical lens, we established a 1 mm thick sheet of laser light with an approximately 35 degree opening angle (Fig. 1). The laser beam was guided by an optical fiber. A beam stabilizer was used to eliminate small fluctuations in the power output of the laser. Prior to ignition, the gas phase above the open top fuel surface was seeded with talc particles with a mean diameter of 3 ± 1 μm determined by scanning electron microscope.

The trajectories of these particles were recorded by a high speed video camera which was connected to a video system and a TV monitor for the real time observation of both flow field and spreading flame.

Dual Wavelength Holographic Interferometry (DWHI)

The basic principles behind DWHI are the same as those for the single HI [4–6]. A schematic of DWHI is shown in Fig. 5. DWHI is an indirect measurement technique with a response time of less than a microsecond and a spatial resolution of less than $\pm$ 0.1 mm in identifying concentration difference. The DWHI has significant advantages over the microsampling technique, which has a spatial resolution of several millimeters and a response time that is at best on the order of a second. In addition, the microsampling technique is a direct technique that will cause a large physical disturbance in the flow field [16].

In the present study we use a 2–D model of DWHI and experimentally determine the best possible 2–D condition for the measurement. Details will be given in the following section. Because the basic principles of DWHI are detailed in [17, 18], we will provide only the equations for the temperature and the fuel concentration, respectively.

$$T = \frac{(3P/2R)\,[N_{A\lambda_1}(N_B-N_A)_{\lambda_2} - N_{A\lambda_2}(N_B-N_A)_{\lambda_1}]}{[(n-1)_{\lambda_1}(N_B-N_A)_{\lambda_2} - (n-1)_{\lambda_2}(N_B-N_A)_{\lambda_1}]}\,.$$

$$C = \frac{[(n-1)_{\lambda_2}N_{A\lambda_1} - (n-1)_{\lambda_1}N_{A\lambda_2}]}{[(n-1)_{\lambda_1}(N_B-N_A)_{\lambda_2} - (n-1)_{\lambda_2}(N_B-N_A)_{\lambda_1}]}\,.$$

The symbols N and n–1 in these equations are respectively defined as:

$$N = X_{fuel}N_{fuel} + (1 - X_{fuel})N_{air}$$

and

$$n{-}1 = 3/2(P/RT)[N_{air} + X_{fuel}(N_{fuel} - N_{air})].$$

The other symbols are: T = temperature, X_i = mole fraction of species i, P = pressure, M_i = molar refractivity of species i, R = universal gas constant for fuel vapor, W_i = molecular weight of species i, λ_1 = wavelength of laser beam 1 (Green Ar–ion laser–beam), and λ_2 = wavelength of laser beam 2 (He–Ne laser–beam).

DW holograms contain holograms of two different wavelengths that need to be separated, one corresponding to the temperature difference and the other to the density difference. We first recorded the holograms on a high sensitivity film. Then, during the printing process, two different filters were used to separate the two holograms. These filters have narrow band–pass widths, each passing the wavelength match to that of its respective laser–beam.

RESULTS AND DISCUSSION

PTLS Results

A schematic of the pulsating flame spread consisting of six different steps is shown in Fig. 2. Step (a) is the beginning of the cycle of pulsation and the process moves on to steps (b), (c), (d_1), (d_2) , (e), and returns to step (a) to complete the cycle. The schematic of step (d_1), not shown in the original diagram published in 1991 [4], was added because it helps us understand the process of flame pulsation better.

At both steps (a) and (b), the flame is at rest and heat is transferred from the flame to the liquid; step (a) is the initial step and (b) represents a further developed state such that the size of the liquid–convection cell at (b) is larger than that at (a). During this preheating process, the temperature difference in the liquid increases as a function of time setting up step (c). At step (c), the temperature difference in the liquid became large enough to generate a surface tension driven flow, i.e., when the original liquid convection CCZ reached a certain mean diameter, it produced a new liquid convection, STF. The thickness of STF is approximately one third that of CCZ. Just after STF is generated, the flame suddenly moved forward (step d_1) indicating that the fuel concentration ahead of the flame's leading edge satisfied the lean flammable limit (the assumption of the formation of the lean flammable mixture is important, thus we measured it by DWHI). When the flame reached the head of CCZ, it stopped (step d_2). A few seconds later, the step (e) took place. Then the process returned to the step (a). The holograms corresponding to the steps (a), (b), (c), (d_1) and (e) were published in [4]. Five different vector diagrams corresponding to 2–D flow under the conditions of (a, b, c, d_1, and d_2) in Fig. 2 are shown in Figs. 3. The flow diagram for step (e) is not shown, because it is similar to that of step (a). Figure 4 shows a vector diagram for a 2–D flow obtained in the uniform spread region, and the corresponding schematic of the uniform spread. All the flow diagrams mentioned here (Figs. 3 a–d and 4) were obtained from the high speed video films and were averaged over at least several trials (reproducibility was excellent).

Figures 3 (a) and (b) do not show any circulation in the gas phase. When the process progressed to Fig. 3 (c), an interesting result occurred: a millimeter–diameter circulation in the gas phase between the flame's leading edge and the liquid surface appeared. At the same time, the aluminum particles on the liquid also moved forward indicating the initiation of liquid convection (likely a surface tension driven flow). This process is also schematically depicted in Fig. 2. When the flame moved forward again, the processes corresponding to the small gas–phase circulation, Figs. 3 (d_1) and (d_2), disappeared. Thus, our experimental results agree very well with the theoretical predictions made by Schiller and Sirignano [11,12]. We also conducted the same experiment in the uniform spread region and no clear gas–phase circulation was obtained (Fig. 4). However, a vector diagram of the flow (Fig. 4) shows the existence of a source of expansion, which is located just ahead of the the flame's leading edge. This indicates the possibility of existence of a small gas–phase circulation. This possibility will be further investigated in the future.

DWHI Results

High speed video and IR photographs taken from above the tray revealed that for the 0.5 cm wide tray, both the surface–temperature distribution and the shape of the flame front are parabolic in nature, while for the 1, 2 and 4 cm wide trays, small twin circulations were generated on the fuel surface [10] suggesting that the character of the flow profile of the gas phase flow profile is changed from 2D to 3D by increasing the width of the tray. A recent study by Garcia–Ybarra [19] also suggested the 3–D nature of the gas–phase flow induced by a spreading flame over alcohols. To increase the accuracy of the DWHI, the 3–D effect needs to be minimized. We experimentally did this by taking a series of video pictures together with DW holograms and identifying the best 2–D–flame shape from the video film and corresponding DW hologram.

Figure 6 shows a combined DW hologram in the uniform spread region, and Fig. 7 shows two different holograms: (a) an Ar–Ion–laser–beam hologram, and (b) a He–Ne–laser–beam hologram obtained in the pulsating spread region. Figure 8 shows profiles of the temperature and propanol concentration obtained from the holograms of Fig. 7 in the pulsating flame–spread region corresponding to Fig. 3 (c). Figure 8 shows that the propanol concentration in the propanol–air mixture just ahead of the flame's leading edge is within the lean flammability limit. This verifies the assumption made by both Glassman and Dryer [7] that the mechanism of pulsating flame spread is the alternation of two different flame–spread processes: the flame spread in a premixed gas layer and the flame spread driven by a subsurface–liquid convection. We also obtained two DW holograms: one corresponding to the condition of Fig. 2 (a) and the other corresponding to Fig. 2 (b), and applied the same procedure to obtain propanol concentrations in the gas phase just ahead of the flame's leading edge. We found that the mole fraction of propanol in the propanol–air mixture was less than 2.2%, which was below the lean flammability limit.

Again our result confirms the pulsating spread mechanism proposed by Glassman and Dryer [7].

It should be noted that our DWHI assumes a 2–D model and the pulsating flame spread consists of spreads by a blue finger (or clawing) flame and a main luminous flame, in which the finger–flame spread is rather unstable. The applicability of the 2–D–model assumption to this flame needs to be further investigated.

SUMMARY AND CONCLUSIONS

(1) Previously, we developed a unique PTLS system for measuring velocity profiles for transient flow in a very limited space. We applied this PTLS system to study the mechanism of the pulsating flame spread over propanol and successfully obtained a series of PTLS flow diagrams. These PTLS flow diagrams revealed a gas–phase circulation on the order of 1–mm diameter in the pulsating spread region together with a liquid–phase convection, both of which were predicted by other researchers.

(2) Gas–flow profiles induced by a spreading flame over the liquid change from 2D to 3D with increasing tray width. Accordingly, the structure of the liquid convection may change by increasing the tray width. Thus the effect of the tray width on the spread mechanism needs to be investigated in the future.

(3) We applied the DWHI system to measure transient profiles of the gas–phase–propanol concentration over the liquid–propanol surface. We obtained a series of DW holograms and confirmed that the flame spread occurred only when the propanol concentration is within the lean flammability limit. Our current DWHI assumes a 2–D model, thus the accuracy of the DWHI needs to be improved when it is applied to 3–D problems.

(4) Our DWHI results also show that the mechanism of pulsating flame spread over propanol consists of two different processes: a flame spread through a lean flammable propanol–air mixture and a flame spread driven by a subsurface–liquid convection. Our DWHI also show that the propanol concentration just ahead of the flame's leading edge is within the lean flammability limit. This is further evidence that in the uniform spread

region the subsurface–liquid convection exists and generates a flammable propanol–air mixture above the fuel surface.

ACKNOWLEDGEMENTS

This study was supported in part by the National Institute of Standards and Technology under Grant #60NANB4D1674, in part by the NASA–Kentucky EPSCoR Program, in part by the Japanese Ministry of Education under US–Japan Collaborative Agreement Travel Grant, and in part by the Center for Manufacturing Systems at the University of Kentucky under a matching grant. We would like to thank H. Ross and F. Miller of NASA Lewis Research Center for providing us with their experimental data and many stimulating discussions.

REFERENCES

1. Ross, H.D., **Prog. Energ. Combust. Sci.**, 20: 17–63 (1994).

2. Hirano, T., and Suzuki, T., **Fire Safety J.**, 21: 207–229 (1993).

3. Williams, F.A., **Combustion Theory, Second Edition,** Benjamin/Cumming, Menlo Park, CA, (1985), Chap. 12.

4. Ito, A, Masuda, D, and Saito, K., **Combust Flame**, 83: 375–389 (1991).

5. Ito, A., Saito, K., and Cremers, C.J., "Pulsating Flame Spread over Liquids," **Fire Safety Science – Proc. Fourth International Symposium,** Edited by T. Kashiwagi, International Association for Fire Safety Science, (1995), pp. 445–456.

6. Tashtoush, G., Narumi, A., Ito, A., Saito, K., and Cremers, C.J., Combined Techniques of Holographic Interferometry and Particle Track Laser Sheet to Study Flame Spread over Liquids," **Eighth International Symposium of Application of Fluid Mechanics,** Lisbon, Portugal, (1996).

7. Glassman, I. and Dryer, F.L., **Fire Safety Journal,** 3: 123–138 (1981).

8. Akita, K., "Some Problems of Flame Spreading along a Liquid Surface," **Fourteenth Symposium (International) on Combustion,** The Combustion Institute, (1972), pp. 1075–1083.

9. Miller, F.J. and Ross, H.D., "Further Observation of Flame Spread over Laboratory–Scale Alcohol Pools," **Twenty–Fourth Symposium (International) on Combustion,** The Combustion Institute, (1992), pp. 1703–1711.

10. Ross, H., and Miller, F.J., "Detailed Experiments of Flame Spread Across Deep Butanol Pools," **Twenty–Sixth Symposium (International) on Combustion,** The Combustion Institute, (1996), to appear.

11. Schiller, D.N. and Sirignano, W.A., **J. Thermophys. Heat Transfer.**, 6: 105–130 (1992).

12. Sirignano, W.A. and Schiller, D.N., **Combust. Sci. Tech.**, (1996), to appear.

13. Santoro, R.J., Fernandez–Pello, A.C., Dryer, F.L., and Glassman, I., **Appl. Optics,** 17: 3843 (1978).

14. Venkatesh, S, Ito, A, Saito, K., and Wichman, I.S., "Anchoring Mechanism of Liquid Pool Fires," **Twenty–Sixth Symposium (International) on Combustion,** The Combustion Institute, (1996), to appear.

15 Hirano, T., and Saito, K., **Prog. Energ. Combust. Sci.,** 20: 461–485 (1995).

16. Saito, K., Williams, F.A., and Gordon, A.S., **J. Heat Transfer,** 108: 640–648 (1986).

17. Spatz, T.L, and Poulikakos, D., **J. Heat Transfer,** 114: 998 (1992)

18. Ito, A., Narumi, A., Saito, K. and Cremers, C.J., "Temperature Measurement in Liquids by Holographic Interferometry," **Proc. Eighth International Symposium on Transport Phenomena on Combustion,** S.H. Chan Edit., (1995), to appear.

19. Garcia–Ybarra, P.L., et al., "Study of the Thermocapillary Layer Preceding Slow Steadily–Spreading Flames over Liquid Fuels," **Twenty–Sixth Symposium (International) on Combustion,** The Combustion Institute, (1996), to appear.

Figure Captions

Figure 1 Experimental apparatus of Particle–Track Laser–Sheet (PTLS) system connected to a high speed camera, VCR and TV monitor. Nitrogen was used for flame extinguishment and the particle seeding system is the same as the one used previously (see [14]). The thermocouple was used to measure the initial liquid temperature.

Figure 2 Schematics of the pulsating flame spread. The original schematics were published in 1991 [4]. STF stands for a surface tension flow, and CCZ for the cold convective zone. This time, an additional step (d_2) was added to the original five step (a through e) process.

Figure 3 Five different PTLS flow diagrams obtained in the pulsating flame spread region over propanol. The initial liquid temperature: 13. 8^{o}C and the ambient air temperature: 19.2 ^{o}C. The captions: (a) through (d_2) correspond to the conditions described in Fig. 2.

Figure 4 A PTLS flow diagram obtained in the uniform spread region over propanol and a schematic of the uniform flame spread process. The initial liquid temperature was: 18.4^{o}C and the ambient air temperature was: 22.4^{o}C.

Figure 5 A schematic of DWHI system.

Figure 6 A DW hologram obtained in the uniform spread region (the experimental condition is the same as Fig. 4).

Figure 7 Two holograms: (a) an Ar–ion laser beam hologram and (b) a He–Ne laser beam hologram, separated from a DW hologram obtained in the pulsating spread region (the experimental .

Figure 8 Vertical profiles of (a) gas–phase temperature and of (b) mole fraction of propanol, both constructed from the Figs 5 and 6 holograms at two different locations specified in Fig. 6.

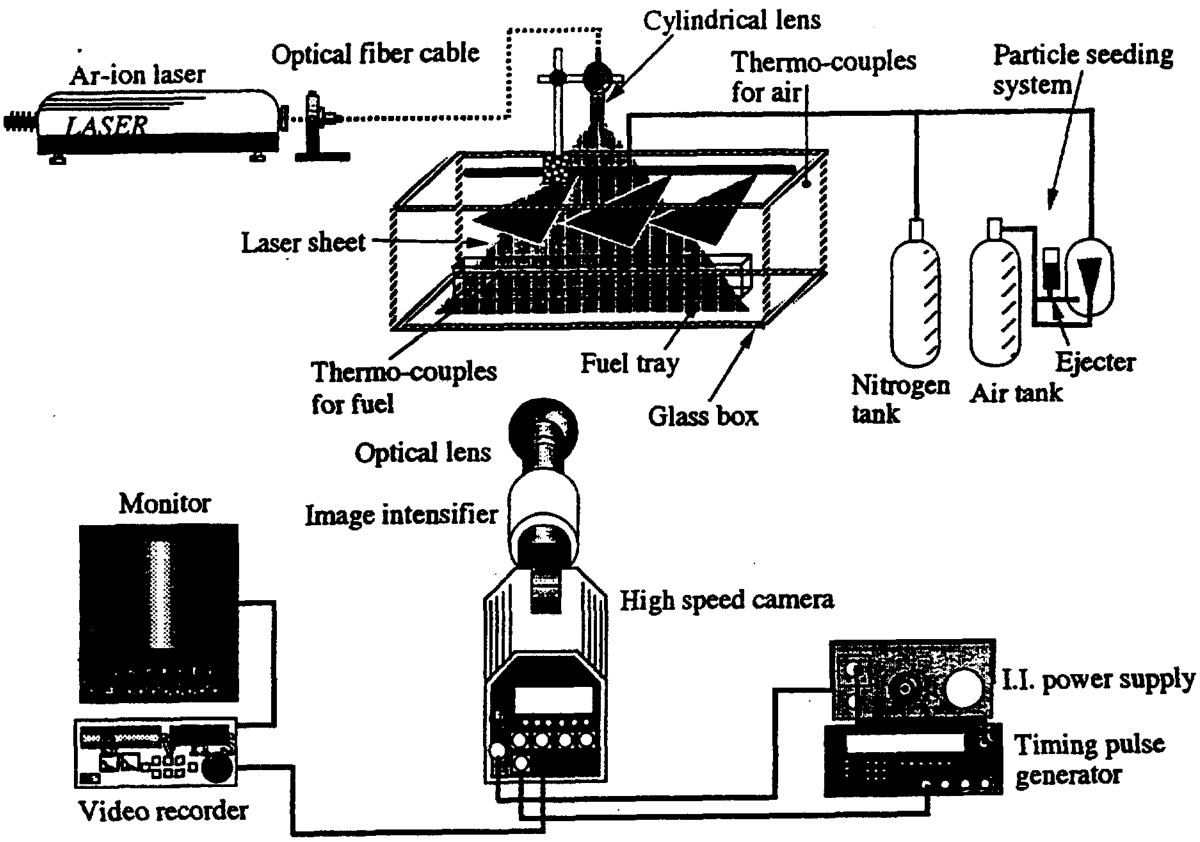

Ito et al - Fig1

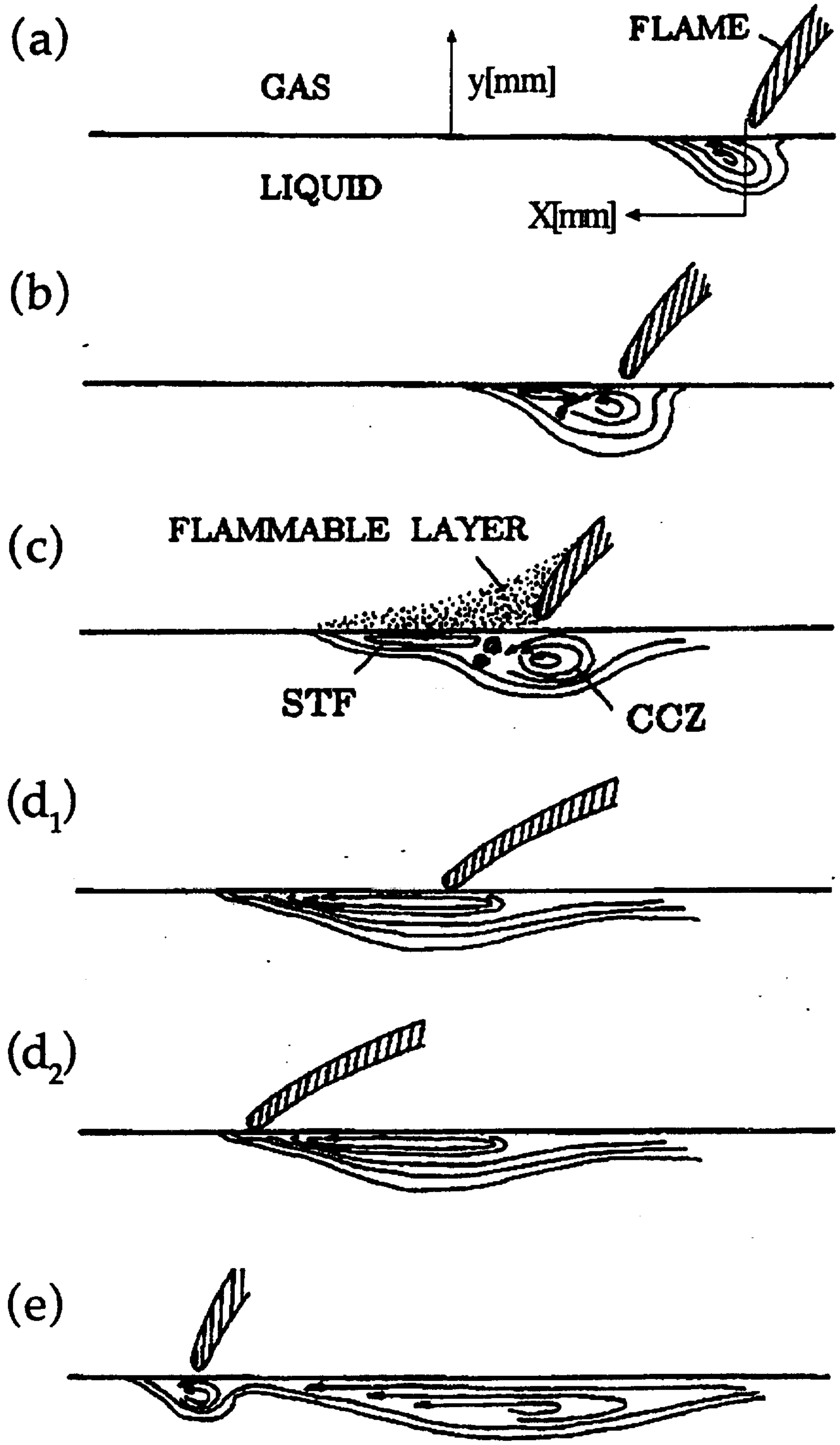

Ito et al - Fig2

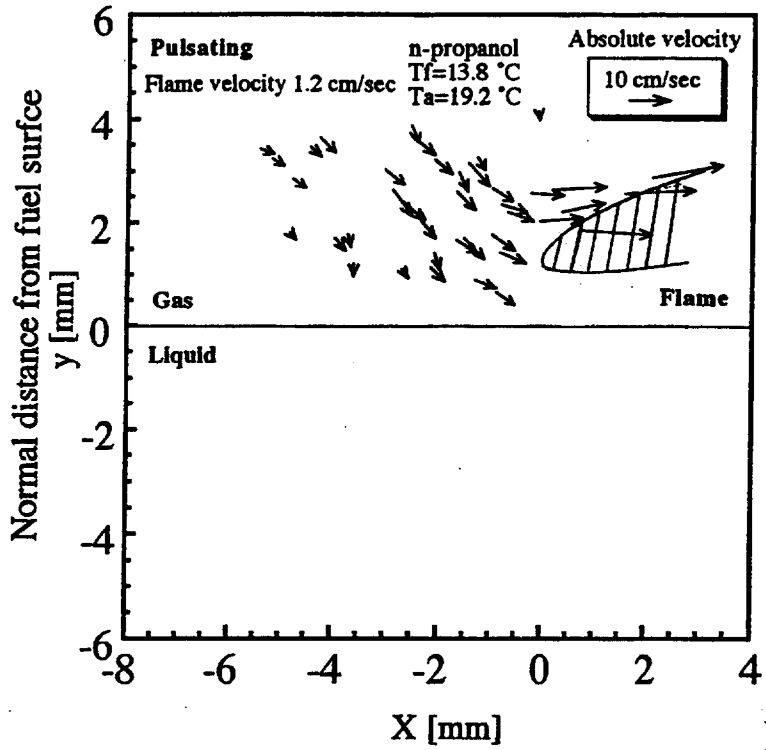

Ito et al - Fig3(a)

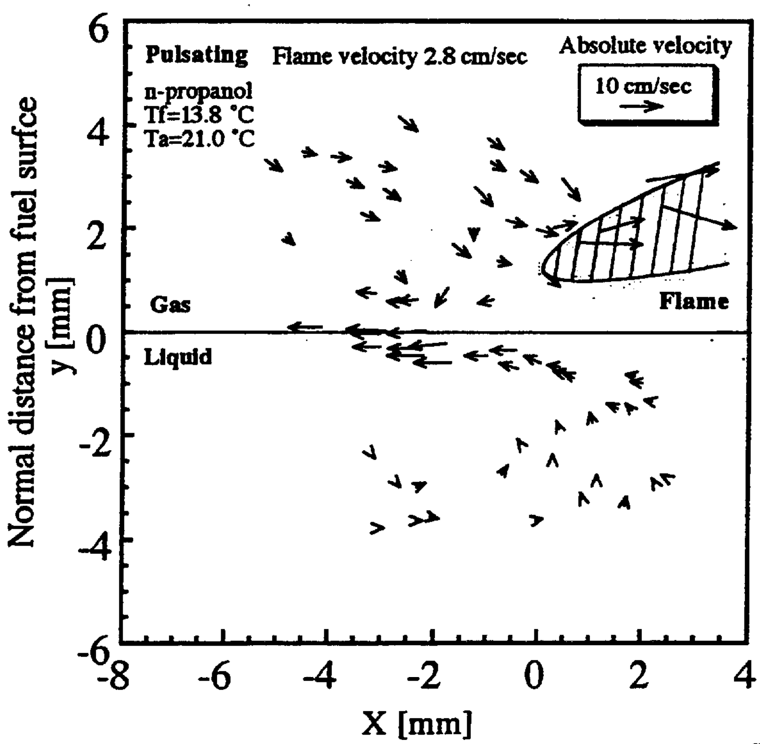

Ito et al - Fig3(b)

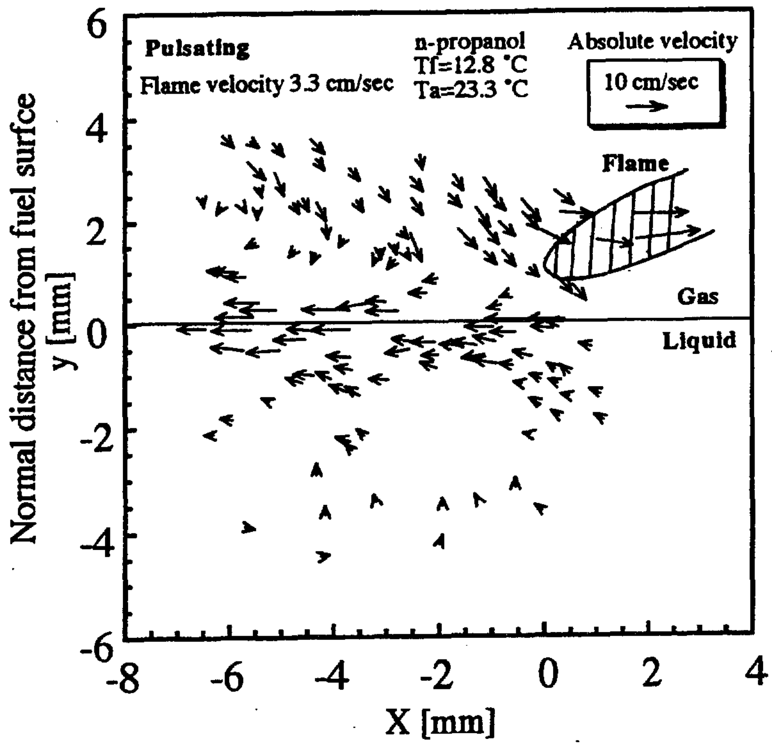

Ito et al - Fig3(c)

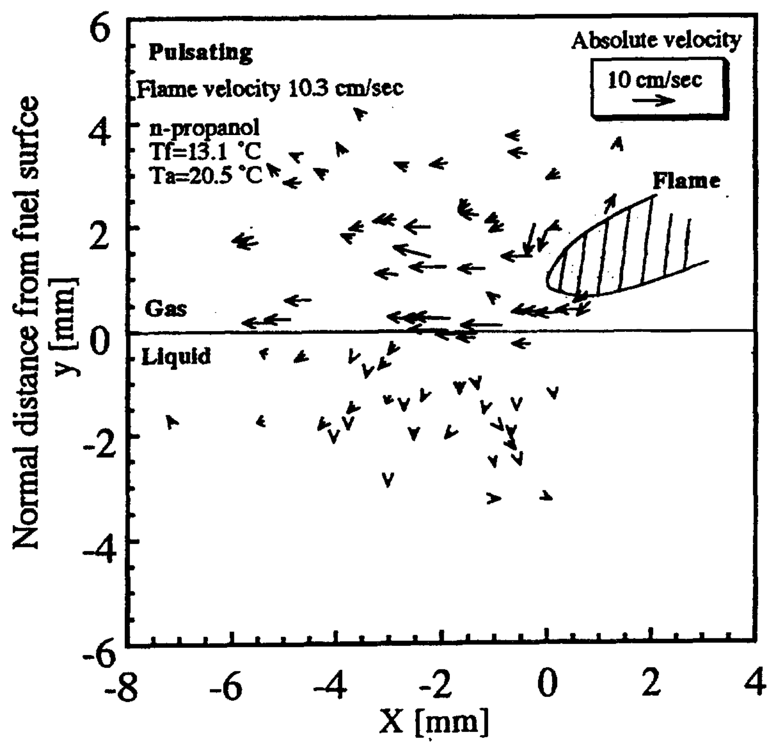

Ito et al - Fig3(d_1)

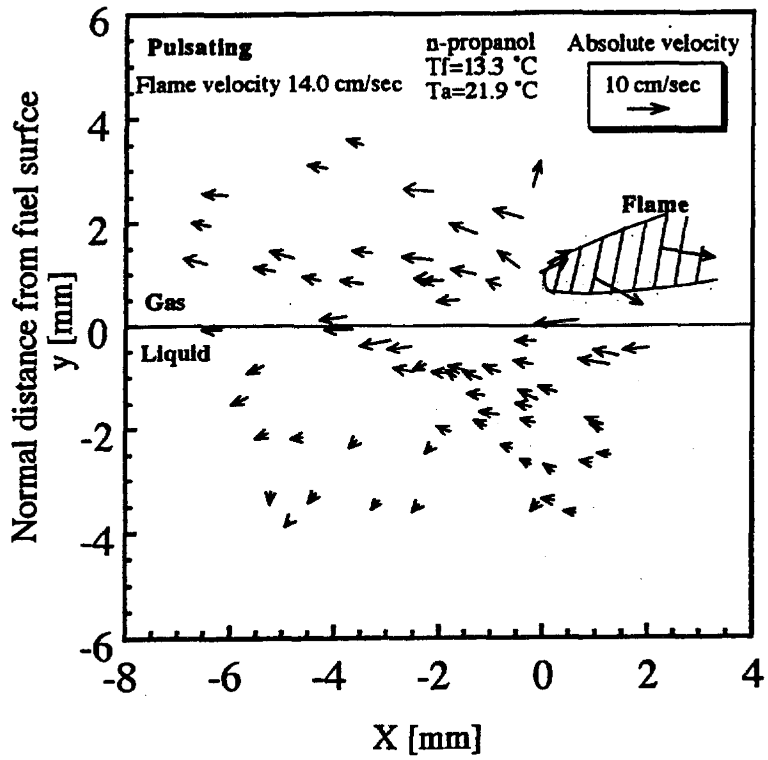

Ito et al - Fig3(d_2)

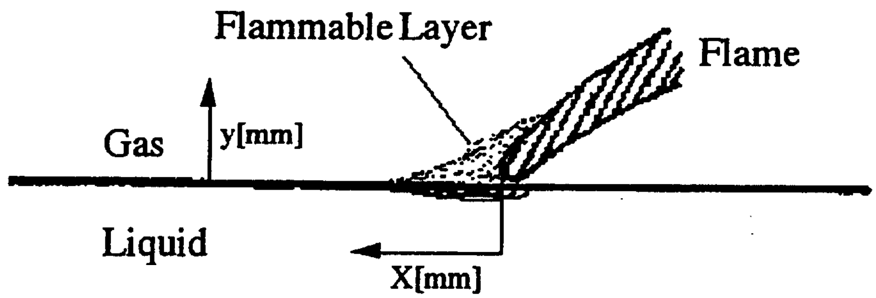

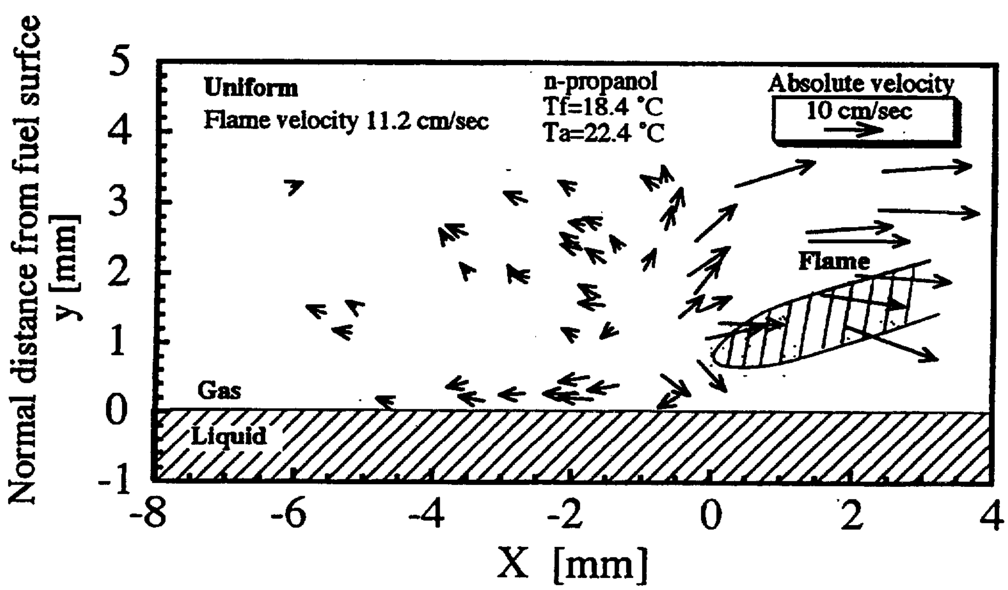

Ito et al - Fig4

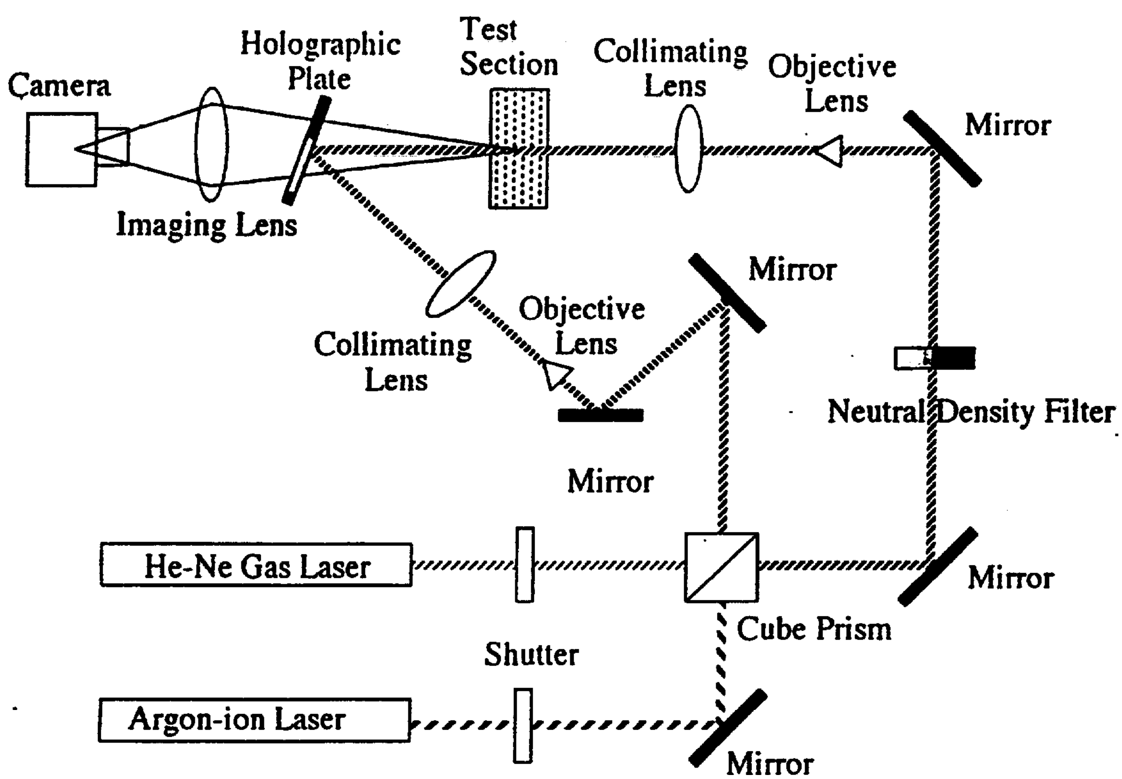

Ito et al - Fig5

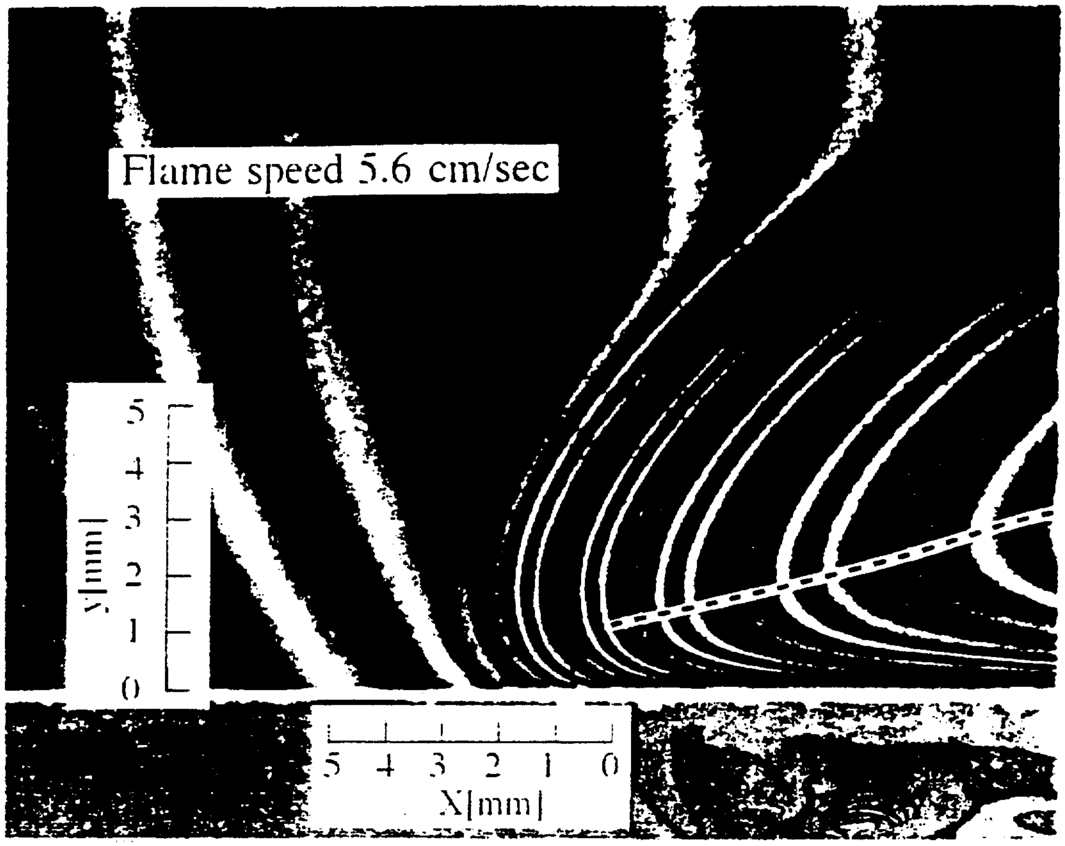

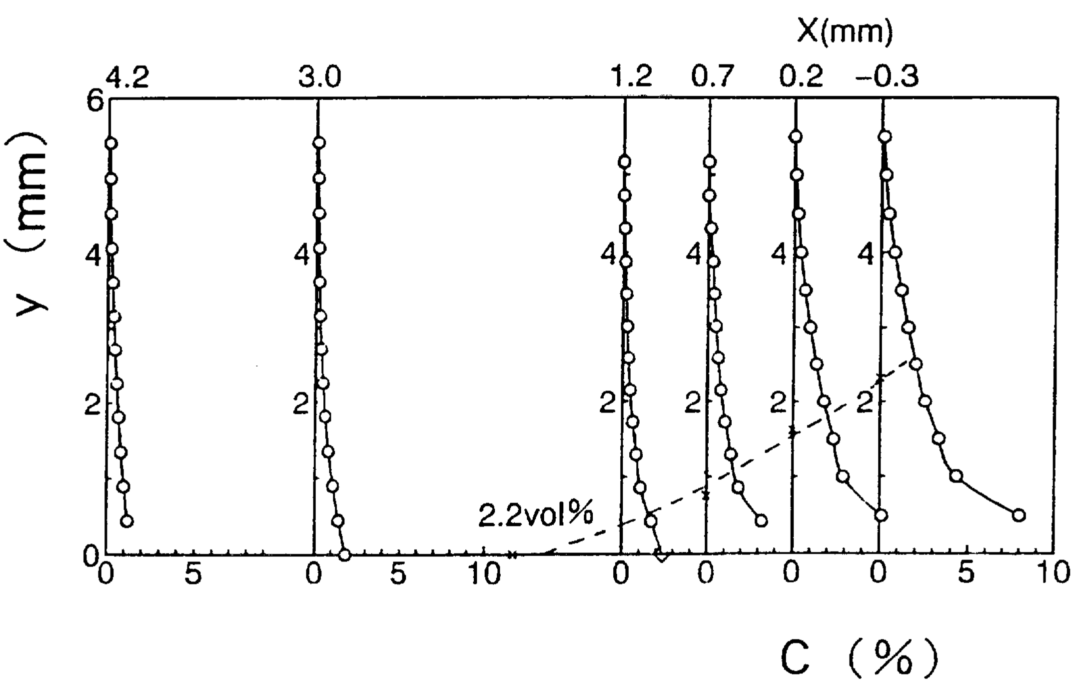

Ito et al - Fig6

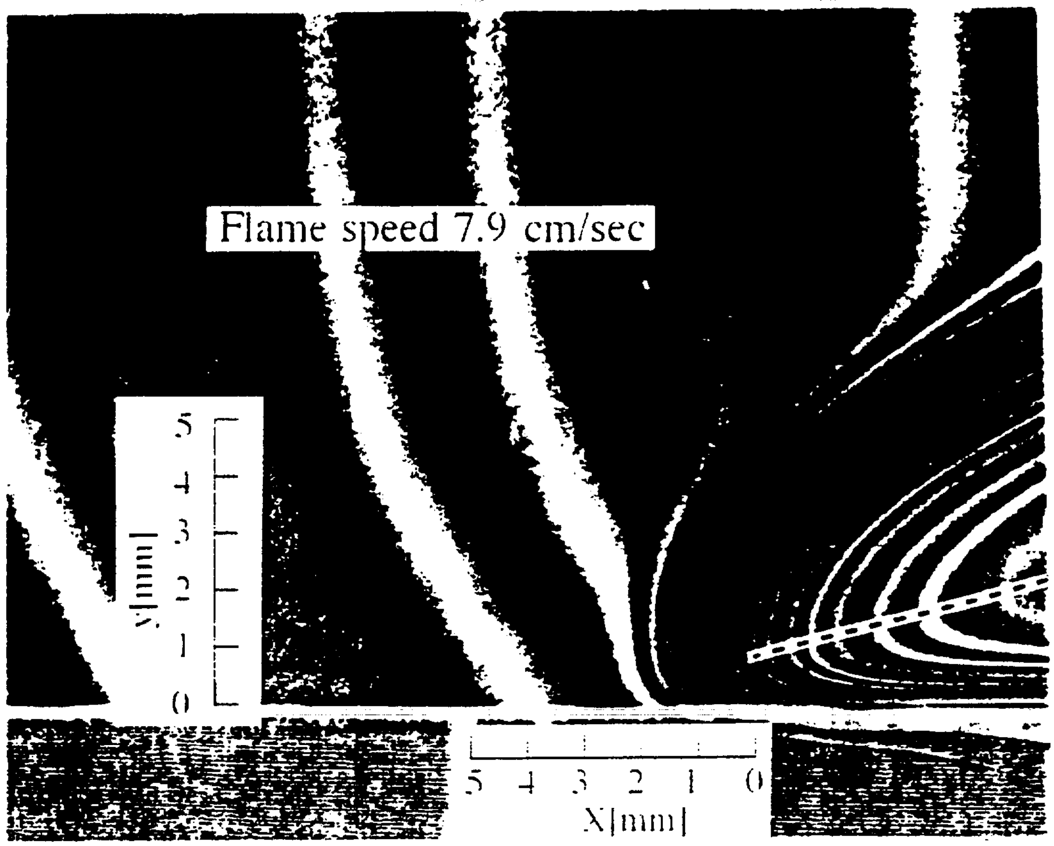

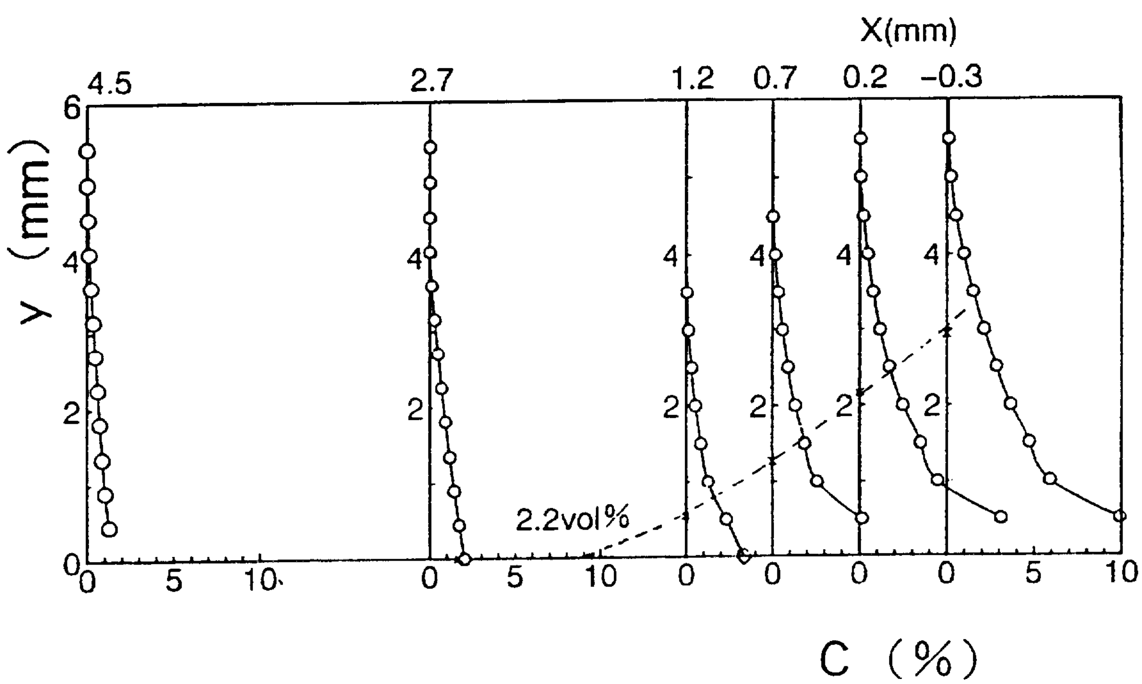

Ito et al - Fig7

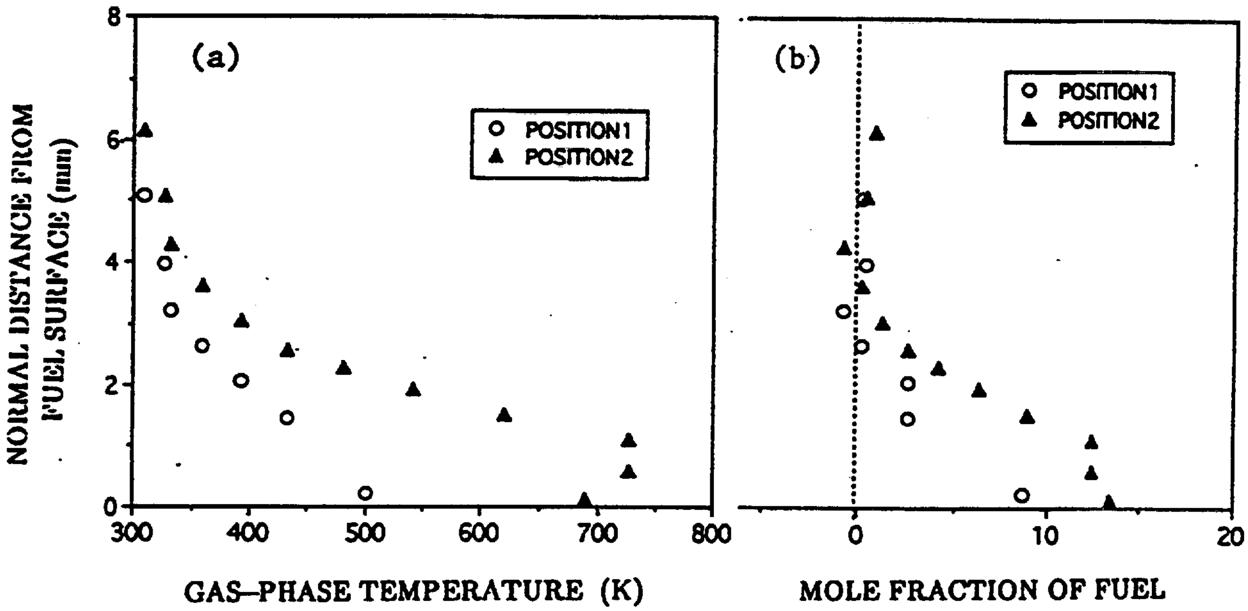

Ito et al – Fig. 8